Search for $\nu_\mu \rightarrow \nu_\tau$ oscillation with the OPERA experiment in the CNGS beam

2012 New J. Phys. 14 033017

(http://iopscience.iop.org/1367-2630/14/3/033017)

New Journal of Physics
The open-access journal for physics

Search for $\nu_\mu \rightarrow \nu_\tau$ oscillation with the OPERA experiment in the CNGS beam

N Agafonova[1], A Aleksandrov[2,40], O Altinok[3], A Anokhina[4], S Aoki[5], A Ariga[6], T Ariga[6], D Autiero[7], A Badertscher[8], A Bagulya[9], A Ben Dhahbi[6,10], A Bertolin[11], C Bozza[12], T Brugière[7], R Brugnera[11,13], F Brunet[14], G Brunetti[7,15,16], S Buontempo[2], A Cazes[7], L Chaussard[7], M Chernyavskiy[9], V Chiarella[17], A Chukanov[18], N D'Ambrosio[19], F Dal Corso[11], Y Déclais[7], P del Amo Sanchez[14], G De Lellis[2,20], M De Serio[21], F Di Capua[2], A Di Crescenzo[2,20], D Di Ferdinando[16], N Di Marco[19], S Dmitrievski[18], M Dracos[22], D Duchesneau[14], S Dusini[11], T Dzhatdoev[4], J Ebert[23], O Egorov[24], R Enikeev[1], A Ereditato[6], L S Esposito[8], J Favier[14], T Ferber[23], R A Fini[21], D Frekers[25], T Fukuda[26], A Garfagnini[11,13], G Giacomelli[15,16], M Giorgini[15,16,41], C Göllnitz[23], J Goldberg[27], D Golubkov[24], L Goncharova[9], Y Gornushkin[18], G Grella[12], F Grianti[17,28], A M Guler[3], C Gustavino[19,42], C Hagner[23], K Hamada[29], T Hara[5], M Hierholzer[23], A Hollnagel[23], K Hoshino[29], M Ieva[21], H Ishida[26], K Ishiguro[29], K Jakovcic[30], C Jollet[22], F Juget[6], M Kamiscioglu[3], S H Kim[31,43], M Kimura[26], N Kitagawa[29], B Klicek[30], J Knuesel[6], K Kodama[32], K Kogiso[29], M Komatsu[29], U Kose[11], I Kreslo[6], C Lazzaro[8], J Lenkeit[23], I Lippi[11], A Ljubicic[30], A Longhin[17], P Loverre[33], G Lutter[6], A Malgin[1], G Mandrioli[16], K Mannai[10], J Marteau[7], T Matsuo[26], V Matveev[1], N Mauri[15,16,44], E Medinaceli[16], F Meisel[6], A Meregaglia[22], P Migliozzi[2], S Mikado[26], S Miyamoto[29], P Monacelli[34], K Morishima[29], U Moser[6], M T Muciaccia[21,35], N Naganawa[29], T Naka[29], M Nakamura[29], T Nakano[29], Y Nakatsuka[29], D Naumov[18], V Nikitina[4], K Niwa[29], Y Nonoyama[29], S Ogawa[26], N Okateva[9], A Olshevsky[18], T Omura[29], O Palamara[19], M Paniccia[17,45], A Paoloni[17], B D Park[31,46], I G Park[31], A Pastore[21,35], L Patrizii[16], E Pennacchio[7], H Pessard[14,39], C Pistillo[6], N Polukhina[9], M Pozzato[15,16], K Pretzl[6], F Pupilli[34], R Rescigno[12], T Roganova[4], H Rokujo[5], G Romano[12], G Rosa[33], I Rostovtseva[24], A Rubbia[8],

A Russo[2], V Ryasny[1], O Ryazhskaya[1], O Sato[29], Y Sato[37], A Schembri[19], W Schmidt-Parzefall[23], L Scotto Lavina[2,47], A Sheshukov[18], H Shibuya[26], G Shoziyoev[4], S Simone[21,35], M Sioli[15,16], C Sirignano[12], G Sirri[16], J S Song[31], M Spinetti[17], L Stanco[11], N Starkov[9], M Stellacci[12], M Stipcevic[30], T Strauss[6], P Strolin[2,20], K Suzuki[29], S Takahashi[5], M Tenti[15,16], F Terranova[17,36], I Tezuka[37], V Tioukov[2], P Tolun[3], A Trabelsi[10], T Tran[7], S Tufanli[6], P Vilain[38], M Vladimirov[9], L Votano[17], J L Vuilleumier[6], G Wilquet[38,39], B Wonsak[23], V Yakushev[1], C S Yoon[31], J Yoshida[29], T Yoshioka[29], Y Zaitsev[24], S Zemskova[18], A Zghiche[14] and R Zimmermann[23]
(The OPERA Collaboration)

[1] INR—Institute for Nuclear Research of the Russian Academy of Sciences, RUS-117312 Moscow, Russia
[2] INFN Sezione di Napoli, I-80125 Napoli, Italy
[3] METU—Middle East Technical University, TR-06531 Ankara, Turkey
[4] SINP MSU—Skobeltsyn Institute of Nuclear Physics, Lomonosov Moscow State University, RUS-119992 Moscow, Russia
[5] Kobe University, J-657-8501 Kobe, Japan
[6] Albert Einstein Center for Fundamental Physics, Laboratory for High Energy Physics (LHEP), University of Bern, CH-3012 Bern, Switzerland
[7] IPNL, Université Claude Bernard Lyon 1, CNRS/IN2P3, F-69622 Villeurbanne, France
[8] ETH Zurich, Institute for Particle Physics, CH-8093 Zurich, Switzerland
[9] LPI—Lebedev Physical Institute of the Russian Academy of Sciences, 119991 Moscow, Russia
[10] Unité de Physique Nucléaire et des Hautes Energies (UPNHE), Tunis, Tunisia
[11] INFN Sezione di Padova, I-35131 Padova, Italy
[12] Dipartimento di Fisica dell'Università di Salerno and INFN, I-84084 Fisciano, Salerno, Italy
[13] Dipartimento di Fisica dell'Università di Padova, I-35131 Padova, Italy
[14] LAPP, Université de Savoie, CNRS/IN2P3, F-74941 Annecy-le-Vieux, France
[15] Dipartimento di Fisica dell'Università di Bologna, I-40127 Bologna, Italy
[16] INFN Sezione di Bologna, I-40127 Bologna, Italy
[17] INFN—Laboratori Nazionali di Frascati dell'INFN, I-00044 Frascati (Roma), Italy
[18] JINR—Joint Institute for Nuclear Research, RUS-141980 Dubna, Russia
[19] INFN—Laboratori Nazionali del Gran Sasso, I-67010 Assergi (L'Aquila), Italy
[20] Dipartimento di Scienze Fisiche dell'Università Federico II di Napoli, I-80125 Napoli, Italy
[21] INFN Sezione di Bari, I-70126 Bari, Italy
[22] IPHC, Université de Strasbourg, CNRS/IN2P3, F-67037 Strasbourg, France
[23] Hamburg University, D-22761 Hamburg, Germany

[24] ITEP—Institute for Theoretical and Experimental Physics, RUS-317259 Moscow, Russia
[25] University of Münster, D-48149 Münster, Germany
[26] Toho University, J-274-8510 Funabashi, Japan
[27] Department of Physics, Technion, IL-32000 Haifa, Israel
[28] Università degli Studi di Urbino 'Carlo Bo', I-61029 Urbino, Italy
[29] Nagoya University, J-464-8602 Nagoya, Japan
[30] IRB—Rudjer Boskovic Institute, HR-10002 Zagreb, Croatia
[31] Gyeongsang National University, ROK-900 Gazwa-dong, Jinju 660-701, Korea
[32] Aichi University of Education, J-448-8542 Kariya (Aichi-Ken), Japan
[33] Dipartimento di Fisica dell'Università di Roma 'La Sapienza' and INFN, I-00185 Roma, Italy
[34] Dipartimento di Fisica dell'Università dell'Aquila and INFN, I-67100 L'Aquila, Italy
[35] Dipartimento di Fisica dell'Università di Bari, I-70126 Bari, Italy
[36] Dipartimento di Fisica dell'Università di Milano-Bicocca, I-20126 Milano, Italy
[37] Utsunomiya University, J-321-8505 Tochigi-Ken, Utsunomiya, Japan
[38] IIHE, Université Libre de Bruxelles, B-1050 Brussels, Belgium
E-mail: Henri.Pessard@lapp.in2p3.fr and Gaston.Wilquet@ulb.ac.be

New Journal of Physics **14** (2012) 033017 (17pp)
Received 17 October 2011
Published 13 March 2012
Online at http://www.njp.org/
doi:10.1088/1367-2630/14/3/033017

Abstract. The OPERA neutrino experiment in the underground Gran Sasso Laboratory (LNGS) was designed to perform the first detection of neutrino oscillations in direct appearance mode in the $\nu_\mu \rightarrow \nu_\tau$ channel, the ν_τ signature being the identification of the τ-lepton created in its charged current interaction.

[39] Authors to whom any correspondence should be addressed.
[40] On leave of absence from LPI—Lebedev Physical Institute of the Russian Academy of Sciences, 119991 Moscow, Russia.
[41] Present address: INAF/IASF, Sezione di Milano, I-20133 Milano, Italy.
[42] Present address: Dipartimento di Fisica dell'Università di Roma 'La Sapienza' and INFN, I-00185 Roma, Italy.
[43] Present address: Pusan National University, Geumjeong-Gu Busan 609-735, Korea.
[44] Present address: INFN—Laboratori Nazionali di Frascati dell'INFN, I-00044 Frascati (Roma), Italy.
[45] Present address: LAPP, Université de Savoie, CNRS/IN2P3, F-74941 Annecy-le-Vieux, France.
[46] Present address: Asan Medical Center, 388-1 Pungnap-2 Dong, Songpa-Gu, Seoul 138-736, Korea.
[47] Present address: SUBATECH, CNRS/IN2P3, F-44307 Nantes, France.
[48] Present address: Albert Einstein Center for Fundamental Physics, Laboratory for High Energy Physics (LHEP), University of Bern, CH-3012 Bern, Switzerland.

The hybrid apparatus consists of a large mass emulsion film/lead target complemented by electronic detectors. Placed in the LNGS, it is exposed to the high-energy long-baseline CERN Neutrino beam to Gran Sasso (CNGS) 730 km away from the neutrino source. The observation of a first ν_τ candidate event was reported in 2010. In this paper, we discuss the result of the analysis of the data taken during the first two years of operation (2008–2009) underlining the major improvements brought to the analysis chain and to the Monte Carlo simulations. The statistical significance of the one event observed so far is then evaluated to 95%.

Contents

1. Introduction

Neutrino oscillations were first predicted nearly 50 years ago [1] and were definitely established in 1998 by the super-Kamiokande experiment with atmospheric neutrinos [2]. Several other experiments carried out in the last two decades with atmospheric, solar, reactor and accelerator neutrinos have established our current understanding of neutrino mixing and oscillations (see e.g. for a review [3]). In particular, the depletion in the ν_μ neutrino flux through oscillation observed by several atmospheric neutrino experiments [2, 4] was confirmed by two accelerator experiments [5]. The fact that the $\nu_\mu \to \nu_e$ oscillation cannot be the dominant channel has been indirectly confirmed by two nuclear reactor experiments [6]. An indication of the appearance of ν_e in a ν_μ beam with a statistical significance of 2.5σ has recently been published by the T2K experiment [7]. However, a direct flavour transition has not yet been established where the oscillated neutrino is identified by the charged lepton created in its CC interaction. The appearance of ν_τ in an accelerator ν_μ beam will unambiguously prove that $\nu_\mu \to \nu_\tau$ oscillation is the dominant transition channel for the neutrino atmospheric sector. This is the main goal of the long-baseline OPERA experiment [8, 9], with its detector exposed in the Gran Sasso Underground Laboratory (LNGS) to the high-energy CERN CNGS neutrino beam [10].

The detection of CNGS neutrino interactions in OPERA was reported in [11] and the observation of a first ν_τ candidate event was presented in [12]. In this paper, we summarize the major improvements brought to the analysis chain and to the Monte Carlo simulations. They mainly concern the evaluation of the efficiencies and the reduction or better control of the physics backgrounds. Event statistics acquired during the first two years of data-taking in 2008 and 2009 and corresponding to 4.88×10^{19} protons on target (p.o.t.) are used for the studies reported here. The statistical significance of the observation of one ν_τ candidate event reported in [12] is re-assessed.

2. The OPERA detector and the CNGS beam

The challenge of the OPERA experiment is to achieve the very high spatial accuracy required for the detection of τ leptons (whose decay length is of the order of 1 mm in this experiment) inside a large-mass active target. The hybrid detector [13] is composed of two identical super modules (SM), each consisting of an instrumented target section of a mass of about 625 tons followed by a magnetic muon spectrometer. A target section is a succession of walls filled with elements called bricks, interleaved with planes of scintillator strips composing the target tracker (TT) that triggers the read-out and allows localizing neutrino interactions within the target. A brick is an emulsion cloud chamber module consisting of 56 1-mm-thick lead plates interleaved with 57 nuclear emulsion films. It weighs 8.3 kg and its thickness corresponds to ten radiation lengths along the beam direction. Tightly packed removable doublets of emulsion films called changeable sheets (CS) are glued to the downstream face of each brick. They serve as interfaces between the TT planes and the bricks to facilitate the location of neutrino interactions. Large brick-handling ancillary facilities are used to bring emulsion films from the target up to the automatic scanning microscopes in Europe and Japan. Extensive information on the OPERA detector and facilities is given in [13–15].

OPERA is exposed to the long-baseline CNGS ν_μ beam [10], 730 km away from the source. The beam is optimized for the observation of ν_τ CC interactions. The average neutrino energy is $\sim$17 GeV. In terms of interactions, the $\bar{\nu}_\mu$ contamination is 2.1%, the ν_e and $\bar{\nu}_e$ contaminations are together lower than 1%, while the intrinsic ν_τ component in the beam is negligible.

3. Location of neutrino interactions

The expected number of neutrino events registered in the target volume is 850 per 10^{19} p.o.t. per 1000 tons. A 10% error is assigned to this number resulting from uncertainties on the neutrino flux and interaction cross-sections. During the 2008 and 2009 runs, the average target mass was 1290 tons, of which 8.6% was dead material other than lead plates and emulsion films. The total number of p.o.t was 1.78×10^{19} in 2008 and 3.52×10^{19} in 2009, respectively.

With a trigger efficiency of 99%, the total numbers of triggers in 2008 and 2009 on-time with the beam amount to 10 121 and 21 455, respectively. About 85% of these are due to particles entering the target after being emitted in neutrino interactions occurring in the rock surrounding or in material inside the LNGS cavern. This component, hereafter called ‘external events’, was identified during the 2008 run by performing a visual inspection of all on-time events. Events with topologies consistent with charged particles entering the detector or with low-energy interaction of neutrons and γ-rays, mimicking a neutral current (NC) interaction, were discarded from the sample. For the 2008 data, stringent criteria were used, guaranteeing a high level of purity at the cost of some inefficiency for very low activity events. A total of 1698 events was retained and constitutes the 2008 sample. In 2009, events compatible with occurring in the target volume were selected by an automatic algorithm [16, 17] developed on the basis of the experience acquired with the 2008 sample. The automatic procedure reduces the human workload required by the visual inspection. It also aims at reaching higher efficiency for a specific category of signal events: τ emitted in quasi-elastic (QE) interactions decaying to an electron have a topology very similar to external NC-like events. The drawback is an increased number of external events to be measured.

A Monte Carlo simulation including both external events and interactions occurring inside the target well reproduces the experimental data for what concerns the event rates and position distribution inside the target, validating the automatic selection algorithm. This is particularly true for the low-energy external NC-like events which accumulate close to the target borders. The efficiency of the algorithm is estimated by simulation to be 96.2 and 86.3% for CC and NC events, respectively. The contamination by external events, lower than 1% for CC events, is 23.3% for NC events. By applying the automatic selection algorithm on the 2009 sample, 3629 events were expected from the simulation and 3693 were eventually retained from the experimental data. The sample was further reduced to 3557 events after visual inspection of the event displays.

Data from the electronic detectors associated with the 5255 events reconstructed as occurring inside the target volume were processed by a software algorithm that selects the brick with the highest probability to contain the neutrino interaction vertex. The brick so designated is removed from the target, the CS is detached and its films are searched for tracks compatible with the electronic data to verify the brick selection. In the case this search is unsuccessful, the brick is equipped with a fresh CS and reinserted into the target. A second brick is then extracted according to its probability to contain the vertex complemented by a visual inspection of the event display. In the case the search is successful the brick is dismounted and the emulsion films are dispatched to the scanning laboratories. All tracks measured with high precision in the CS films are sought in the most downstream films of the brick. These tracks are then followed back until they are not found in three consecutive films. A volume is then scanned around their stopping point in order to localize the interaction vertex.

4. Search for decay topologies: the observation of a first ν_τ candidate event

Preserving a high selection efficiency for the QE $\tau \rightarrow e$ channel at the cost of a larger contamination of external events does not increase significantly the number of interaction vertices located in the target (consisting mainly of ν_μ CC and NC events). This number can therefore be predicted by relying only on the size of the essentially uncontaminated 2008 sample. From the 1698 events constituting the 2008 sample, a fraction of about 5% of the events was rejected because of occurring in bricks equipped with poor-quality emulsion films, 1000 interaction vertices were located in bricks and 110 in the dead material. The resulting vertex location efficiencies are 74 ± 2 and 48 ± 4% for CC and NC ν_μ interactions, respectively. By rescaling for the integrated p.o.t., the expected number of located events to be searched for decays of short-lived particles in the entire 2008 and 2009 samples is 2978 ± 75. More information on detection efficiencies for signal events is given in section 5.

The results presented in this paper concern the decay search analysis of 2738 events, i.e. 92% of the total 2008 and 2009 event sample. The bias on efficiency estimations the lack of the remaining 8% of events may induce, if any, is negligible. In the analysed sample, which corresponds to a total of 4.88×10^{19} p.o.t., 81% of events have an identified muon in the final state.

Table 1. Selection criteria for ν_τ candidate events as set in [9] and the corresponding values measured for the first observed tau-candidate event [12].

Variable	Cut-off	Value
Missing p_T at the primary vertex (GeV/c)	<1.0	$0.57^{+0.32}_{-0.17}$
Angle between the parent track and the primary hadronic shower in the transverse plane (rad)	$>\pi/2$	3.01 ± 0.03
Kink angle (mrad)	>20	41 ± 2
Daughter momentum (GeV/c)	>2	12^{+6}_{-3}
Daughter p_T when γ-ray at the decay vertex (GeV/c)	>0.3	$0.47^{+0.24}_{-0.12}$
Decay length (μm)	<2 lead plates	1335 ± 35

In order to analyse the primary vertex a volume scan is performed over a 1 cm^2 area in at least two films upstream and six films downstream of the vertex lead plate. A procedure was developed to detect charged and neutral decays as well as secondary interaction and γ-ray conversion vertices in the vicinity of the primary vertex; it was introduced in [12] and detailed in [18].

When a secondary vertex is found the kinematical analysis of the whole event is performed. This analysis uses the values of the angles measured in the emulsion films, of the momenta determined by multiple Coulomb scattering measured in the brick, of the momenta measured by the magnetic spectrometers and of the total energy deposited in the instrumented target acting as a calorimeter [12, 17, 19]. The energy of γ-rays and electrons is estimated by a neural network algorithm that uses the combination of the number of track segments in the emulsion films and the shape of the electromagnetic shower, together with the multiple Coulomb scattering of the leading tracks.

By applying this procedure, one ν_τ candidate event was observed, as reported in detail in [12]. We recall that the tau-candidate event had seven prongs at the primary vertex, out of which four are identified as originating from a hadron and three have a probability lower than 0.1% of being caused by a muon, none being left by an electron. The parent track exhibits a kink topology and the daughter track is identified as produced by a hadron through its interaction. Its impact parameter with respect to the primary vertex is (55 ± 4) μm; the impact parameter is smaller than 7 μm for the other tracks. Two γ-rays point to the secondary vertex. The event passes all the selection cuts defined in the experiment proposal and summarized in table 1 [9].

The invariant mass of the two γ-rays is $(120 \pm 20(\text{stat.}) \pm 35(\text{syst.}))$ MeV/c^2, consistent with the π^0 mass. Together with the secondary hadron assumed to be a π^- they have an invariant mass of $(640^{+125}_{-80}(\text{stat.})^{+100}_{-90}(\text{syst.}))$ MeV/c^2. The decay mode is therefore compatible with being $\tau \to \rho^-(770)\nu_\tau$, whose branching ratio is about 25%. The statistical significance of this event was estimated to be 98.2%, as the probability that it was not due to a fluctuation of the background simulating a decay in the $\tau \to h$ channel [12].

5. Signal detection efficiencies and physics background

The validity of the Monte Carlo simulation of the electronic detectors response has been verified through a detailed comparison with experimental data. This comparison concerns the muon

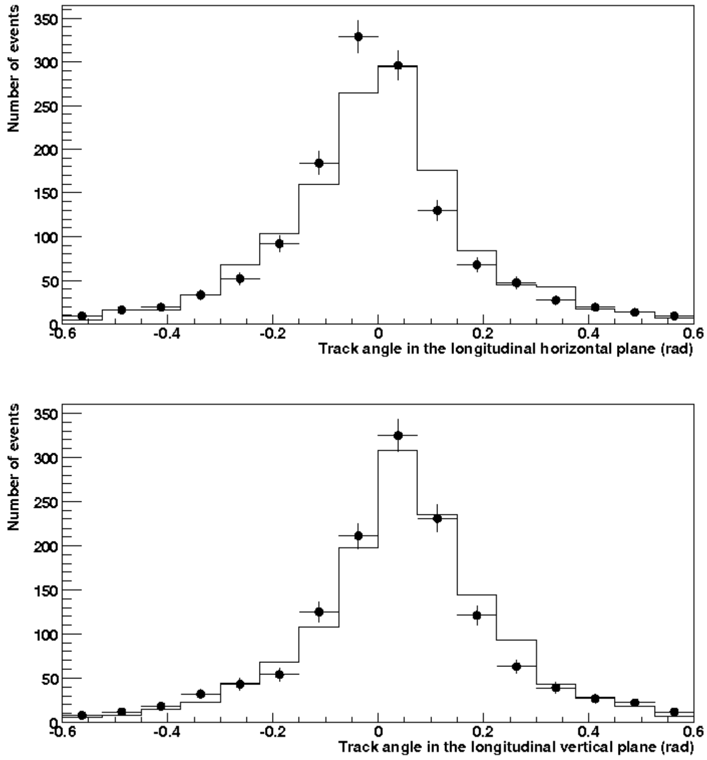

Figure 1. Angle of tracks reconstructed at the primary vertex in the longitudinal horizontal (top) and vertical (bottom) planes: comparison between experimental data (lines with error bars) and simulated data (continuous line).

identification and the reconstruction of its momentum and charge, as well as the reconstruction of the total energy and the hadronic shower profile [17]. The event simulation and the off-line reconstruction software have been extended to the response of the emulsion films, allowing all the algorithms used in the analysis of real events to be applied to simulated data. This includes scanning of the CS films, track connection between CS films and downstream films of the brick and track following towards the vertex. The subsequent scan of a volume around the vertex is complemented by track following from the vertex and searching for secondary decay or interaction vertices and for electromagnetic showers [20]. Simulation and off-line reconstruction algorithms have been successfully implemented up to the events topology and their location inside the bricks. The agreement between experimental and simulated data is shown in figures 1 and 2. Further work is in progress with the aim of a full, data-driven simulation of all scanning and analysis phases.

Charged charmed particles have lifetimes similar to that of the τ lepton and share analogous decay topologies. The finding efficiency of the decay vertices is therefore also similar for both types of particles. Comparing the observed charm event sample in size, decay topologies and kinematics with expectations from simulations constitutes a straightforward way to verify that prompt-decay selection criteria and their corresponding efficiencies and backgrounds are well understood. Recently published cross-sections have been used in the simulation [20]. The results of this comparison are shown in table 2. Figure 3 shows the distributions of the decay length and of the angle ϕ between the parent track and the primary muon in the plane transverse to the

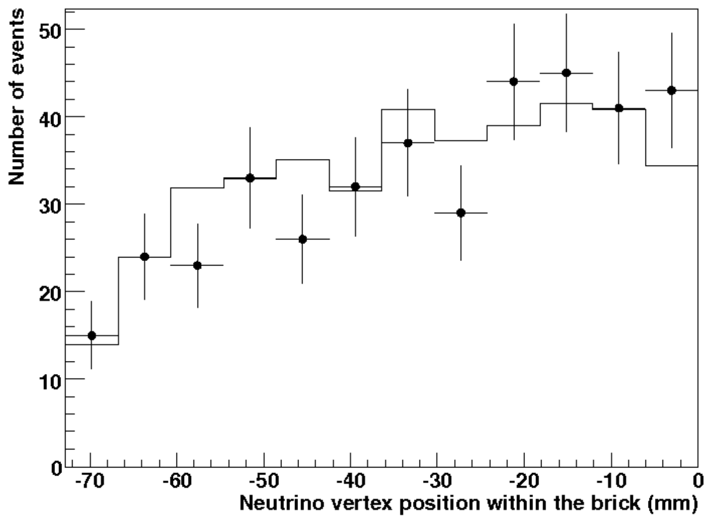

Figure 2. Location within the bricks of the primary vertex of NC events: comparison between experimental data (dots with error bars) and simulated data (continuous line). Most ν_τ CC events have topologies similar to NC events.

Table 2. Comparison of charm event topologies observed and expected from simulations including background.

Topology	Observed charm candidate events	Expected events Charm	Background	Total
Charged one-prong	13	15.9	1.9	17.8
Neutral two-prong	18	15.7	0.8	16.5
Charged three-prong	5	5.5	0.3	5.8
Neutral four-prong	3	2.0	< 0.1	2.1
Total	39	39.1 ± 7.5	3.0 ± 0.9	42.2 ± 8.3

beam direction. There is good agreement between experimental and simulated data both in the number of expected charm events and in the quoted distributions.

The expected numbers of events in the various τ channels for the nominal beam intensity of 22.5×10^{19} p.o.t. in 5 years foreseen in the experiment proposal [9] and for the fraction of the 2008 and 2009 runs analysed so far are shown in table 3. Full mixing and $\Delta m^2_{23} = 2.5 \times 10^{-3}\,\text{eV}^2$ are assumed. The total number of signal events expected to be eventually detected decreased from about 10 as quoted in the experiment proposal [9] to 8, essentially because of the reduced interaction vertex location efficiencies resulting from a more reliable knowledge of the detector and of the analysis procedures. These updated interaction vertex location efficiencies are shown in table 3 together with the global τ detection efficiency that includes the interaction and decay vertices detection efficiencies as well as the selection efficiency to satisfy topological and kinematical criteria at both vertices.

The main source of background to all τ-decay channels is the charged charmed particles that decay into similar channels and are produced in ν_μ CC interactions where the primary muon

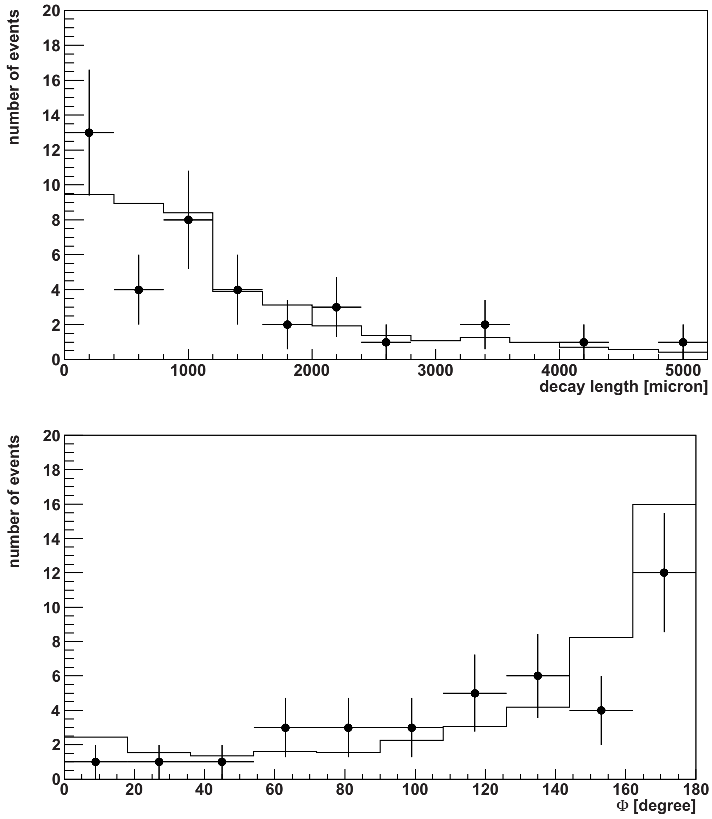

Figure 3. Top: distributions of the decay length of charmed particles for experimental data (dots with error bars) and simulated data (histogram). Bottom: distributions of the angle ϕ between the parent track and the primary muon in the transverse plane of charmed particles for experimental data (dots with error bars) and simulated data (histogram).

is not identified. However, the charmed muon decay channel does not contribute to background if the opposite sign muon charge is correctly measured by the spectrometers. Additional charm background can arise from c–$\bar{c}$ pair production in NC interactions where one charmed particle is not identified, and from $\bar{\nu}_\mu$, ν_e and $\bar{\nu}_e$ CC events that amount to 2.5% in terms of interactions. Second-order effects result from the misidentification of the decay products and the topology.

Identifying the muons coming from the primary vertex with the highest possible efficiency is important for suppressing background. Details of muon identification algorithms based on signals collected by the electronic detectors can be found in [17]; 95% efficiency is reached for the primary muons of charm events. In order to further reduce the muon identification inefficiency, all tracks at the primary interaction of signal candidate events emitted with a polar angle θ smaller than 1 rad are followed within the brick in which the event occurs and from brick to brick. About 30% of muons not identified by the electronic detectors are recovered through the topology of their end-point, range–momentum correlation and energy loss measurement in the last fraction of their range. The residual inefficiency is dominated by muons emitted at angles larger than 1 rad or escaping the target from the side. The technique, in particular,

Table 3. Expected numbers of observed signal events for the design intensity of 22.5×10^{19} p.o.t. and for the 2008 and 2009 analysed data sample corresponding to 4.88×10^{19} p.o.t. The updated efficiency for locating interaction vertices is shown in the fourth column. The last column shows the global τ-detection efficiency that includes detection and selection efficiencies for both interaction and decay vertices as well as the probability to satisfy topological and kinematical criteria at both vertices.

Decay channel	Number of signal events expected for 22.5×10^{19} p.o.t.	Number of signal events expected for 4.88×10^{19} p.o.t.	Interaction vertex location efficiency	Global τ detection efficiency
$\tau \to \mu$	1.79	0.39	0.54	0.09
$\tau \to e$	2.89	0.63	0.59	0.14
$\tau \to h$	2.25	0.49	0.59	0.04
$\tau \to 3h$	0.71	0.15	0.64	0.04
Total	7.63	1.65	0.59	0.07

allows a sizable reduction of the background in the $\tau \to \mu$ channel due to wrong associations of the muons emitted in ν_μ CC events to the vertex of secondary hadronic interactions with kink topologies. This is also true for fake muons in NC events. The hadronic background is also lowered in the $\tau \to h$ channel due to hadron interactions with kink topologies at the primary vertex of ν_μ CC events where the primary muon has escaped identification in the electronic detectors. The technique had been applied in the analysis of the first ν_τ candidate event but not taken into account in the background estimate since the simulation required for assessing it was not available at that time.

The charm background was evaluated using the charm production cross-sections recently published by the CHORUS Collaboration [21]; they are significantly larger than those known at the time of the experiment proposal [9]. The charm production rate induced by neutrinos relative to the CC cross-section is 35% higher at OPERA energies, while the relative charm fragmentation fraction into D^+ increased from 10 to 22%. The overall effect is a charm background increase by a factor of 1.6–2.4 depending on the decay channel.

The second main source of background in the $\tau \to h$ decay channel comes from one-prong inelastic interactions of primary hadrons produced in NC interactions, or in CC interactions where the primary lepton is not identified and in which no nuclear fragments can be associated with the secondary interaction. This has been evaluated with a FLUKA [22]-based Monte Carlo code, as detailed in [12] and cross-checked with three sets of measurements.

Tracks of hadrons from neutrino interactions have been followed far from the primary vertex over a total length of 14 m; this corresponds to the total length of tracks left by hadrons in 2300 NC events. No interactions have been found that fulfil the $\tau \to h$ selection criteria. Immediately outside the signal region, 10 single-prong interactions have been observed with a p_T larger than 200 MeV/c, while 10.8 were expected from simulations. On the top part of figure 4 the total momentum is plotted versus the transverse momentum of the final state particles for these interactions. The parameters space in which τ-decay candidates are accepted is shown.

OPERA-like bricks exposed to 4 GeV/c π^- beams have been analysed in order to further crosscheck the estimate of the hadron interaction background. In a first exposure,

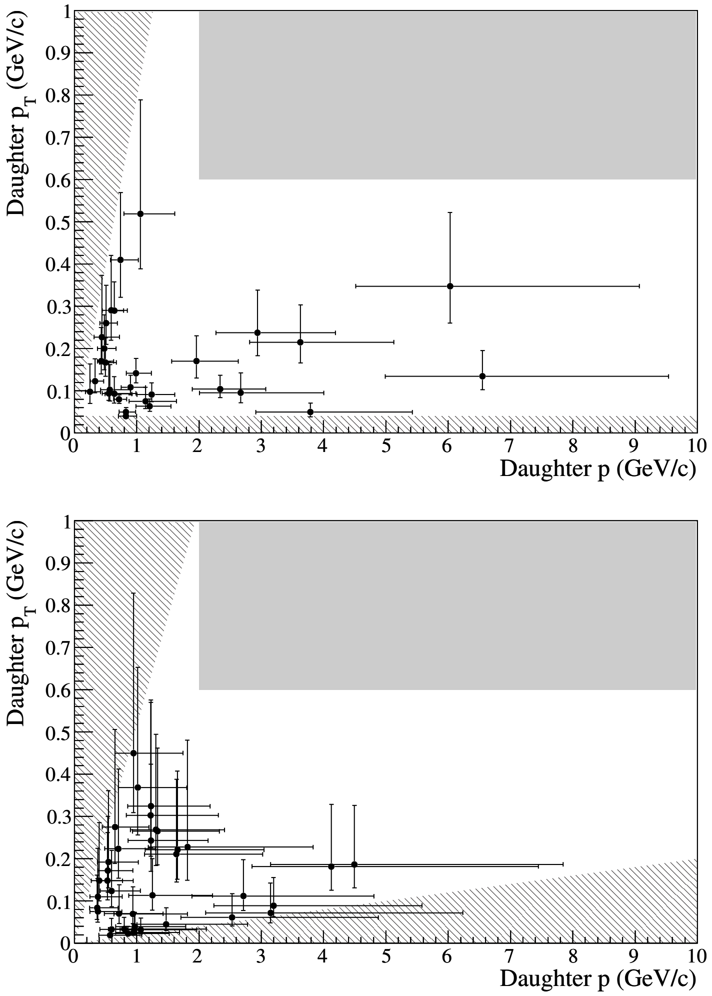

Figure 4. Top: scatter plot of p_T versus p of the daughter particle of single-prong re-interactions of hadrons far from the neutrino interaction vertices where they are produced. Bottom: scatter plot of p_T versus p of the daughter particle of single-prong interactions of 4 GeV/c π^-. On both figures the dark area defines the domain in which τ decay candidates are selected and the hatched area defines the non-physical region $p < p_T$ and the domain rejected by the selection cuts.

314 interactions were localized with an angular acceptance $\theta < 1$ rad, out of which 140 are single-prong events with a kink angle larger than 20 mrad (the same selection cut as for the τ decay search). In a second exposure, 314 interactions were located with an angular acceptance $\theta < 0.54$ rad, out of which 126 are single-prong events with kink angles larger than 20 mrad. On the bottom part of figure 4 the transverse momentum is plotted against the total momentum of the final state particles for the single-prong events in this second exposure. Comparisons showing fair agreement between experimental and simulated data of both exposures are presented in figure 5 for a set of topological variables.

The hadron interactions background can be further reduced by increasing the detection efficiency of highly ionizing particles, low-energy protons and nuclear fragments, emitted in

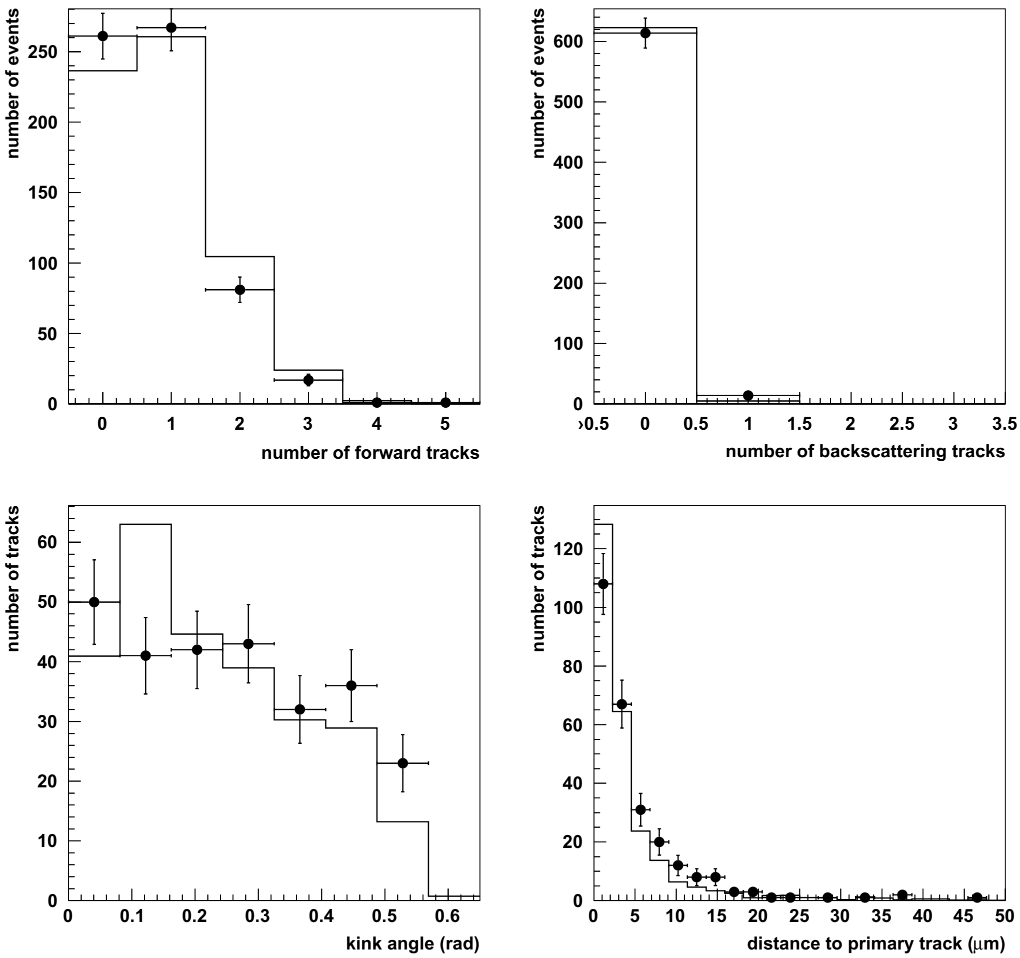

Figure 5. Comparison of experimental data (dots with error bars) and simulation data (histogram) for two bricks exposed to $4\,\mathrm{GeV}/c\,\pi^-$ test beams. Normalizations are independent. Top left: forward tracks multiplicity. Top right: backward tracks multiplicity. Bottom left: kink angle for one-prong events. Bottom right: minimum distance between the primary and the secondary tracks for one-prong events.

the cascade of intra-nuclear interactions initiated by the primary particles and in the nuclear evaporation process. This is a novel feature not yet implemented in the analysis reported in [12]. In order to detect a significant fraction of nuclear fragments emitted at large angle, an image analysis tool was developed. High-resolution microscope tomographic images in 24 layers of $2.5\,\mathrm{mm} \times 2.1\,\mathrm{mm}$ size are analysed in the upstream and downstream films of an interaction vertex. This technique was applied to a sample of 64 interactions in an OPERA-like brick exposed to an $8\,\mathrm{GeV}/c\,\pi^-$ beam. At least one highly ionizing particle was associated with $(56 \pm 7)\%$ of the events with a backward/forward asymmetry of 0.75 ± 0.15, while 53% are expected from simulations with an asymmetry of 0.71. Figure 6 shows fair agreement in polar angle distribution of the highly ionizing particles between experimental and simulated data. The technique allows detecting more highly ionizing particles associated with secondary vertices. It

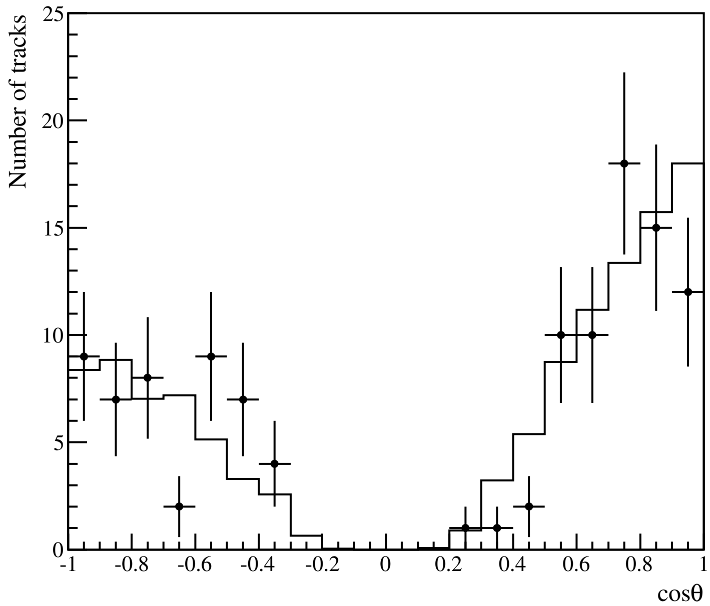

Figure 6. Polar angle distributions of the highly ionizing particles emitted in $8\,\mathrm{GeV}/c\,\pi^-$ interactions in an OPERA-like brick for experimental data (dots with error bars) and simulated data (histogram). Forward tracks correspond to $\cos\theta = 1$.

provides an additional background reduction of about 20%. No such particles were found to be associated with the decay vertex of the first ν_τ candidate event.

The expected background in the muon decay channel caused by large-angle muon scattering has been evaluated in [9].

The total number of expected background events has slightly decreased from 0.75 as quoted in the experiment proposal [9] to 0.73, despite a significant increase of the charm cross-sections, mainly because of a significant improvement in the identification of the decay products as hadron or muon. All background sources are summarized in table 4. Systematic errors of 25% on charm background and of 50% on hadron and muon backgrounds are assumed. Errors arising from the same source are combined linearly and otherwise in quadrature.

6. Signal statistical significance

One ν_τ candidate event is observed in the $\tau \to h$ decay channel that passes all the selection cuts; assuming full mixing and $\Delta m^2_{23} = 2.5 \times 10^{-3}\,\mathrm{eV}^2$ 0.49 ± 0.12 events are expected for this decay mode in the currently analysed sample. The error is estimated close to 25% from the uncertainties on the tau production cross-section and on the detection efficiency. The background in this channel is evaluated to 0.05 ± 0.01(syst) event. The probability for the event to be not due to background fluctuations and thus the statistical significance of the observation is 95%. Considering all decay channels, the numbers of expected signal and background events are, respectively, 1.65 ± 0.41 and 0.16 ± 0.03(syst), the probability for the event to be background being 15%.

Table 4. The expected numbers of observed background events from different sources for the design intensity of 22.5×10^{19} p.o.t. and for the 2008–2009 analysed data sample corresponding to 4.88×10^{19} p.o.t. Errors quoted are systematic.

Decay channel	Number of background events expected for							
	22.5×10^{19} p.o.t.				4.88×10^{19} p.o.t.			
	Charm	Hadron	Muon	Total	Charm	Hadron	Muon	Total
$\tau \to \mu$	0.025	0.00	0.07	0.09 ± 0.04	0.00	0.00	0.02	0.02 ± 0.01
$\tau \to e$	0.22	0.00	0.00	0.22 ± 0.05	0.05	0.00	0.00	0.05 ± 0.01
$\tau \to h$	0.14	0.11	0.00	0.24 ± 0.06	0.03	0.02	0.00	0.05 ± 0.01
$\tau \to 3h$	0.18	0.00	0.00	0.18 ± 0.04	0.04	0.00	0.00	0.04 ± 0.01
Total	0.55	0.11	0.07	0.73 ± 0.15	0.12	0.02	0.02	0.16 ± 0.03

7. Conclusions

The OPERA experiment, aiming at the first detection of neutrino oscillations in direct appearance mode where the oscillated neutrino is identified, completed the study of 92% of the data accumulated during the first two years of operation in the CNGS beam (2008 and 2009), corresponding to an integrated intensity of 4.88×10^{19} p.o.t.

The observation of a single candidate ν_τ event is compatible with the expectation of 1.65 signal events. The significance of the observation of one decay in the $\tau \to h$ channel decreased from 98.2% in the first analysis [12] to 95%, because of the significantly larger size of the analysed event sample.

The anticipated background increase resulting from the recently measured [21] charm cross-sections larger than those known at the time of the experimental proposal was compensated for by a higher muon identification efficiency. In addition, the study of highly ionizing tracks left by protons and nuclear fragments which are often associated with hadronic re-interactions has allowed reducing by about 20% this background specific to the hadronic decay modes of the τ.

The event location efficiency was re-evaluated for several phases of the analysis procedure. The simulation of the event reconstruction at the emulsion film level down to the interaction vertex is at an advanced stage; its completion will help in further checking the detection efficiencies at each step of the analysis process, from the track reconstruction in the electronic detectors to the location of primary and secondary vertices in the emulsion films. This will also allow re-evaluating the selection criteria in view of improving the signal-to-noise ratio.

An analysis of the large event samples collected in the 2010 and 2011 CNGS runs and corresponding to 8.88×10^{19} p.o.t. is in progress.

Acknowledgments

We thank CERN for the successful operation of the CNGS facility and INFN for the continuous support given to the experiment during the construction, installation and commissioning phases through its LNGS laboratory. We warmly acknowledge funding from our national agencies: Fonds de la Recherche Scientifique—FNRS and Institut Interuniversitaire des Sciences Nucléaires for Belgium, MoSES for Croatia, CNRS and IN2P3 for France, BMBF for Germany, INFN for Italy, JSPS (Japan Society for the Promotion of Science), MEXT (Ministry of Education, Culture, Sports, Science and Technology), QFPU (Global COE programme of Nagoya University, Quest for Fundamental Principles in the Universe supported by JSPS and MEXT) and Promotion and Mutual Aid Corporation for Private Schools of Japan for Japan, SNF, the University of Bern and ETH Zurich for Switzerland, the Russian Foundation for Basic Research (grant no. 09-02-00300_a), the Programs of the Presidium of the Russian Academy of Sciences Neutrino physics and Experimental and theoretical researches of fundamental interactions connected with work on the accelerator of CERN, the Programs of Support of Leading Schools (grant no. 3517.2010.2), and the Ministry of Education and Science of the Russian Federation for Russia, the Korea Research Foundation Grant (KRF-2008-313-C00201) for Korea and TUBITAK, the Scientific and Technological Research Council of Turkey, for Turkey. We are also indebted to INFN for providing fellowships and grants to non-Italian researchers. We thank the IN2P3 Computing Centre (CC-IN2P3) for providing computing resources for the analysis and hosting the central database for the OPERA experiment. We are indebted to our technical collaborators for the excellent quality of their work over many years of design, prototyping and construction of the detector and of its facilities.

References

[1] Pontecorvo B 1957 *Zh. Eksp. Teor. Fiz.* **33** 549
Pontecorvo B 1957 *Sov. Phys.—JETP* **6** 429 (Engl. transl.)
Pontecorvo B 1958 *Zh. Eksp. Teor. Fiz.* **34** 247
Pontecorvo B 1958 *Sov. Phys.—JETP* **7** 172 (Engl. transl.)
Maki Z, Nakagawa M and Sakata S 1962 *Prog. Theor. Phys.* **28** 870

[2] Fukuda Y *et al* (SUPER-KAMIOKANDE Collaboration) 1998 *Phys. Rev. Lett.* **81** 1562
Abe K *et al* (SUPER-KAMIOKANDE Collaboration) 2006 *Phys. Rev. Lett.* **97** 171801
Wendell R *et al* (SUPER-KAMIOKANDE Collaboration) 2010 *Phys. Rev.* D **81** 092004

[3] Nakamura K *et al* (Particle Data Group) 2010 *J. Phys.* G **37** 075021

[4] Hirata K S *et al* (KAMIOKANDE-II Collaboration) 1988 *Phys. Lett.* B **205** 416
Ambrosio M *et al* (MACRO Collaboration) 1998 *Phys. Lett.* B **434** 451
Allison W W M *et al* (SOUDAN-2 Collaboration) 2005 *Phys. Rev.* D **72** 052005

[5] Ahn M H *et al* (K2K Collaboration) 2006 *Phys. Rev.* D **74** 072003
Michael D G *et al* (MINOS Collaboration) 2006 *Phys. Rev. Lett.* **97** 191801
Adamson P *et al* (MINOS Collaboration) 2008 *Phys. Rev. Lett.* **101** 221804

[6] Apollonio M *et al* (CHOOZ Collaboration) 2003 *Eur. Phys. J.* C **27** 331
Piepke A (Palo Verde Collaboration) 2002 *Prog. Part. Nucl. Phys.* **48** 113

[7] Abe K *et al* (T2K Collaboration) 2011 *Phys. Rev. Lett.* **107** 041801

[8] Ereditato A, Niwa K and Strolin P 1997 The emulsion technique for short, medium and long baseline $\nu_\mu \rightarrow \nu_\tau$ oscillation experiments **423** INFN-AE-97-06, DAPNU-97-07
Shibuya H *et al* (OPERA Collaboration) 1997 Letter of intent: the OPERA emulsion detector for a long-baseline neutrino-oscillation experiment, CERN-SPSC-97-24, LNGS-LOI-8-97

[9] Guler M *et al* (OPERA Collaboration) 2000 An appearance experiment to search for $\nu_\mu \rightarrow \nu_\tau$ oscillations in the CNGS beam: experimental proposal, CERN-SPSC-2000-028, LNGS P25/2000
Guler M *et al* (OPERA Collaboration) 2001 Status Report on the OPERA Experiment, CERN/SPSC 2001-025, LNGS-EXP 30/2001 add. 1/01

[10] Elsener K 1998 The CERN Neutrino Beam to Gran Sasso (Conceptual Technical Design), CERN 98-02, INFN/AE-98/05

Bailey R *et al* 1999 The CERN Neutrino Beam to Gran Sasso (NGS) (Addendum to Report No. CERN 98-02, INFN/AE-98/05), CERN-SL/99-034(DI), INFN/AE-99/05

[11] Acquafredda R *et al* (OPERA Collaboration) 2006 *New J. Phys.* **8** 303

Agafonova N *et al* (OPERA Collaboration) 2009 *J. Instrum.* **4** P06020

[12] Agafonova N *et al* (OPERA Collaboration) 2010 *Phys. Lett.* B **691** 138

[13] Acquafredda R *et al* (OPERA Collaboration) 2009 *J. Instrum.* **4** P04018

[14] Armenise N *et al* 2005 *Nucl. Instrum. Methods* A **551** 261

De Serio M *et al* 2005 *Nucl. Instrum. Methods* A **554** 247

Arrabito L *et al* 2006 *Nucl. Instrum. Methods* A **568** 578

Morishima K and Nakano T 2010 *J. Instrum.* **5** P04011

[15] Anokhina A *et al* (OPERA Collaboration) 2008 *J. Instrum.* **3** P07002

Anokhina A *et al* (OPERA Collaboration) 2008 *J. Instrum.* **3** P07005

Adam T *et al* 2007 *Nucl. Instrum. Methods* A **577** 523

Nakamura T *et al* 2006 *Nucl. Instrum. Methods* A **556** 80

[16] OPERA Collaboration 2009 OpCarac: an algorithm for the classification of the neutrino interactions recorded by OPERA *OPERA public note 100* http://operaweb.lngs.infn.it:2080/Opera/publicnotes/note100.pdf

[17] Agafanova N *et al* (OPERA Collaboration) 2011 *New J. Phys.* **13** 053051

[18] Ariga A, Ariga T, De Serio M, Di Capua F, Di Crescenzo A and Sato O 2011 The OPERA decay search procedure *OPERA public note 128* http://operaweb.lngs.infn.it:2080/Opera/publicnotes/note128.pdf

[19] Agafanova N *et al* (OPERA Collaboration) 2011 *New J. Phys.* **14** 013026

[20] OPERA Collaboration Neutrino interactions simulation in the ECC bricks of the OPERA experiment, in preparation

[21] Kayis-Topaksu A *et al* (CHORUS Collaboration) 2011 *New J. Phys.* **13** 093002

[22] FLUKA http://www.fluka.org/fluka.php

Battistoni G *et al* 2007 *Proc. Hadronic Shower Simulation Workshop 2006 (Fermilab, 6–8 September 2006)* ed M Albrow and R Raja *AIP Conf. Proc*. **896** 31–49